REPORT DOCUMENTATION PAGE	READ INSTRUCTIONS BEFORE COMPLETING FORM

1. REPORT NUMBER	2. GOVT ACCESSION NO.	3. RECIPIENT'S CATALOG NUMBER
NRL Memorandum Report 4531	AD-A101445	

4. TITLE (and Subtitle)	5. TYPE OF REPORT & PERIOD COVERED
THE STP/S3-4 SATELLITE EXPERIMENT: EQUATORIAL F-REGION IRREGULARITIES	Interim report on a continuing NRL problem.
	6. PERFORMING ORG. REPORT NUMBER

7. AUTHOR(s)	8. CONTRACT OR GRANT NUMBER(s)
M. Singh*, E. P. Szuszczewicz and J. C. Holmes	RR03303

9. PERFORMING ORGANIZATION NAME AND ADDRESS	10. PROGRAM ELEMENT, PROJECT, TASK AREA & WORK UNIT NUMBERS
Naval Research Laboratory Washington, DC 20375	61153N; RR033-02-44; 41-0949-0-1

11. CONTROLLING OFFICE NAME AND ADDRESS	12. REPORT DATE
Office of Naval Research Arlington, VA 22217	July 14, 1981
	13. NUMBER OF PAGES
	16

14. MONITORING AGENCY NAME & ADDRESS(if different from Controlling Office)	15. SECURITY CLASS. (of this report)
	UNCLASSIFIED
	15a. DECLASSIFICATION/DOWNGRADING SCHEDULE

16. DISTRIBUTION STATEMENT (of this Report)

Approved for public release; distribution unlimited.

17. DISTRIBUTION STATEMENT (of the abstract entered in Block 20, if different from Report)

18. SUPPLEMENTARY NOTES

*Present address: Sachs/Freeman Associates, Inc., Bowie, MD 20715 (On leave from Punjabi University, Patiala, India.)

19. KEY WORDS (Continue on reverse side if necessary and identify by block number)

Ionosphere	Equatorial irregularities
"In Situ"	Satellite measurements

20. ABSTRACT (Continue on reverse side if necessary and identify by block number)

The S3-4 "in situ" satellite observations near the nighttime equator (2230 LT) have shown irregularity structures with depletions in plasma density up to 3 orders of magnitude and ranges in horizontal extent from less than 1 km to tens of kms. The holes have sharper gradients on the eastern boundary than across the western counterpart, and the power spectral indices in the irregularities lie between 1.9-2.5 in the intermediate

(Continues)

DD _{FORM} 1473   EDITION OF 1 NOV 65 IS OBSOLETE
1 JAN 73
S/N 0102-014-6601

i

20. ABSTRACT (Continued)

wavelength domain. The east-west assymmetry of the depletions is also shown in the irregularity intensity and spectral strengths. The variations in density are more intense on the western wall of the holes suggesting a scintillation enhancement on the western boundary. In addition, the results of power spectral analyses support the role of the Rayleigh-Taylor instability in the generation of intermediate scale size irregularities during the occurrence of equatorial spread-F.

CONTENTS

THE STP/S3-4 SATELLITE EXPERIMENT:
EQUATORIAL F-REGION IRREGULARITIES

INTRODUCTION

Equatorial F-region irregularities have drawn much interest in recent years because of their undesirable effects on transionospheric communications and their cause-effect relationship with fundamental plasma instability processes. In efforts to understand the causative mechanism(s), considerable advances have been made in areas of detailed ground-based radar observations and "in situ" measurements. The radar observations (e.g., Woodman and La Hoz, 1976; Tsunoda et al. 1979) have found that meter-size irregularities primarily populate the bottomside F-region in the early evening, at later times tend to rise up and break away from their lower altitude source regime and develop structures extending up to the 700-1000 km region. These structures have come to be called "plumes".

On the macroscale (100's of meters to 10's of km) "in situ" nighttime equatorial measurements have revealed large biteouts in plasma density ranging up to three orders of magnitude (Hanson and Sanatani, 1973) and considered just as characteristic of spread-F as the much less intense (meter size) irregularities observed by radar. Later works on biteouts (Brinton et al. 1975; McClure et al. 1977) showed that ion composition inside and outside the holes can be vastly different. The molecular ions can be more abundant inside the holes than outside the holes, and the holes can vary from a few km to tens of km in the horizontal extent.

In examining potential relationships between radar plumes and ionospheric depletions, Szuszczewicz (1978) suggested that equatorial holes and spread-F were the same phenomena with small scale irregularities imbedded within the large scale depletions. He argued that a chemical volume of ion density on the bottomside (containing the signature of bottomside species) could move upward through a stationary neutral atmosphere and appear as biteouts at higher altitudes with much smaller structures (down to the meter range) populating the density gradients which bounded the macroscale depletion. This model was in concert with the numerical results of Scannapieco and Ossakow (1976) and the drift measurements of McClure et al. (1977).

To further study and definitively unfold the detailed relationships between large scale depletions, meter size irregularities and chemical transport processes, a coordinated investigation was conducted which involved simultaneous observations by radar and "in situ" rocket-borne diagnostics (Szuszczewicz et al., 1980). The combined observations have shown that

1

(a) During conditions of well-developed equatorial spread-F the most intense "in situ" irregularities occurred on the bottomside F-layer gradient.

(b) Within a large scale topside F-layer depletion radar backscatter and "in situ" irregularity strengths maximized near the depletion's upper wall.

(c) Ion composition within a topside depletion provided signatures of its bottomside source domain and estimates of average maximum vertical drift velocity. For long-lived depletions, it was found that molecular-ion signatures (NO^+ and O_2^+) can be lost while bottomside levels of N^+ can be maintained when $[O^+] \sim N_e >> [NO^+] + [O_2^+]$; and finally,

(d) Large scale fluctuations of O^+ accompanied by a near-constant level of NO^+ and O_2^+ on the bottomside F-layer gradient suggests that neutral atmospheric turbulence was not a major source for bottomside ionospheric plasma irregularities and the associated triggering of equatorial spread-F.

To complement the vertical profile information provided by the rocket observations, we present and analyze a sample of "in situ" measurements conducted on the STP/S3-4 satellite carrying a pulsed plasma probe experiment. The probe experiment employed a self consistent test for measurement integrity, while determining electron density and temperature as well as density and mean ion mass fluctuations at 5-20 meter resolution. The S3-4 experiment has been discussed by Szuszczewicz et al. (1981). In this paper, we discuss some of the recent results with emphasis on general horizontal morphology, relationships to basic instability processes and associated scintillation effects.

EXPERIMENTAL RESULTS

Plasma Depletions

The data reported here was made available by the NRL-747 paired-pulsed-plasma-probes (P4) experiment (Szuszczewicz et al. 1981) on STP satellite S3-4 in a sun-synchronous orbit at lower F-region altitudes. The satellite crossed the nighttime equator at about 2230 LT when the the frequency of occurrence of spread-F was high. One probe was biased to respond to variations in plasma electron saturation currents ($I_e \propto N_e$) and the other probe responded to the ion saturation

2

currents ($I_i \propto N_e / \sqrt{\overline{M}_i}$). Subject to the selection of a number of commandable modes of operation, either probe could be repetitively pulsed from its fixed-bias level using a special electronic procedure (Holmes and Szuszczewicz, 1975) to generate conventional Langmuir characteristics for full determinations of electron density N_e, temperature T_e and plasma potential V_∞. The different modes of operation and experimental details are discussed by Szuszczewicz et al. (1981).

Figures 1 and 2 present samples of nighttime equatorial irregularity structures as measured by the currents collected by the electron (I_e) and ion (I_i) probes. The Figures show that the holes extend from a few kms to tens of kms, with depletion levels ranging from a factor of 3 (hole A) to a factor of 500 (hole F). A cursory analysis of Figures 1 and 2 reveals three particularly interesting observations:

(a) The density gradients on the opposing sides of each hole are different. Noting that the inclination of the satellite orbit is 96.4° (traveling in the east-to-west direction with time increasing left-to-right) it can be seen that density gradients in holes C-E (Fig. 1) and F (Fig. 2) are sharp on the eastern boundary and soft on each western counterpart. In the case of hole A, B and H (Fig. 1), the density gradients are not quite as sharp in comparison with holes C-F but the average density gradients are still softer on the western boundary. For the holes L (Fig. 1) and N' and L' (Fig. 2), the difference in density gradients on the opposing sides does not constitute any specific behavior while in the hole C' (Fig. 2) the density gradient is sharp on the western boundary. These observations can be summarized by noting that the density gradients are different across the boundaries of each depletion, with a preference for the density gradients to be sharper on the eastern side.

(b) Another interesting feature of the holes is their similarities in structural morphology. Holes A, B and H are similar in their horizontal profiles. A similarity feature can also be identified in the depletion L (Figure 1) and L' (Figure 2). Both of these depletions have a center point (M and M' respectively) around which the structures look similar. At the central point (M and M'), the plasma density approaches the background (undisturbed) level suggesting that one large hole is breaking up or alternatively two smaller ones are merging.

(c) The top panel of Figures 1 and 2 displays relative density fluctuations, $\delta I / I$ determined by variations about
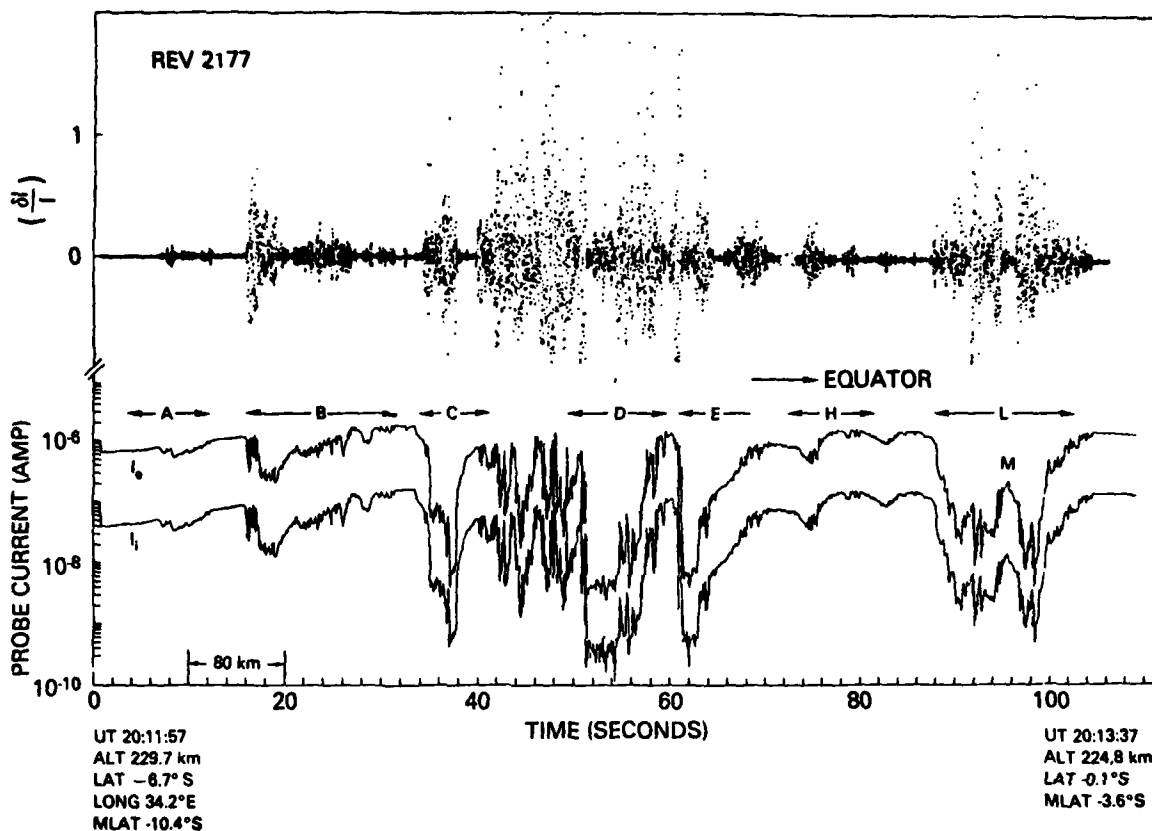
3

Figure 1

Horizontal profile of ionospheric F-region plasma
density as indicated by electron (I_e) and ion (I_i)
saturation currents measured on rev #2177. $\delta I/I$ is
the relative irregularity intensity as calculated
by variations about linear detrends over sliding
2.1 km intervals.

4

Figure 2

Horizontal profile of ionospheric F-region plasma
density as indicated by electron (I_e) and ion (I_i)
saturation currents measured on rev #2470. $\delta I/I$
is the relative irregularity intensity as calculated
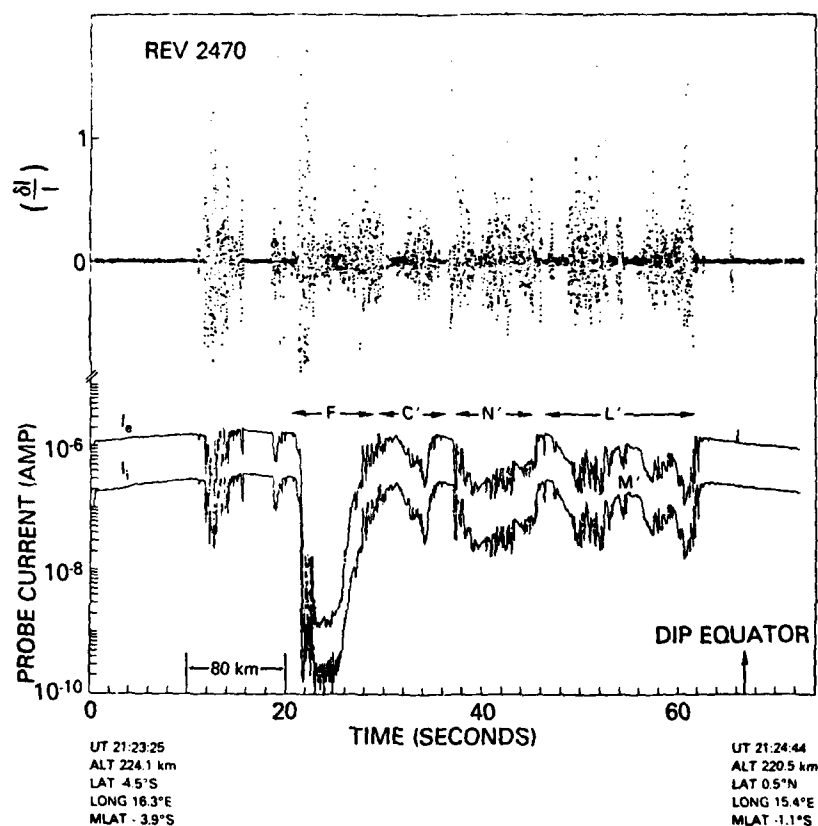by variations about linear detrends over sliding
2.1 km intervals.

5

linear detrends over sliding 2.1 km intervals throughout the
depletions. The fluctuations ($\delta I/I$) easily identifies the
degree of disturbance. The percent variation in the holes
A, B and H (Figure 1) is less than 20% in most parts, while
in other holes of Figures 1 and 2 the variation can be
more than 50%. In addition, the variations can be different
across the opposing boundaries of the holes. We discuss
this more fully below.

East-West Asymmetry

Further illustrations of F-region irregularities appear
in data revs 2122 and 2123 shown in Figure 3. Rev 2123
shows four depletions (numbered 1 through 4) with the depletion
level extending to more than two orders of magnitude. The
rev 2122 shows three depletions (numbered 5 through 7) with
depletions in density up to one order of magnitude.

The discussion is facilitated by identifying certain
features in rev 2123. First, there are clearly defined
regions of undisturbed background ionosphere, marked alphabetically
A through D; the smoothness of the relative density and the
corresponding 0% fluctuations attest to their undisturbed
nature. Focussing on depletions 3 and 4, we see that the
irregularity intensities are 2 to 3 times larger on the
western boundary than on eastern counterparts. This same
relationship is true in depletions 1 and 2, but only after a
qualification that suggests that 1 and 2 are halves of a
larger depletion bounded by A and B. This is supported in
part by the non-existence of a quiescient ionosphere between
the two. When viewed from this perspective the western
boundary is approximately twice as intense in irregularity
intensity as the eastern boundary. In rev 2122, the depletions
6 and 7 show the irregular intensity as more intense on the
western boundary by a factor of 3-4. (On the basis of
similar considerations applied to Figures 1 and 2, we note
that the irregularity intensity is greater on the western
boundaries of depletions D, E and H (Figure 1) and F (Figure
2), while the eastern boundary in holes A-C (Figure 1) is
more intense. Based on irregularity intensity ($\delta I/I$)
observations, we conclude that there is a high probability
of occurrence of more intense fluctuations across the western
boundary of bottomside F-region depletions.

The asymmetry in irregularity strengths and relationships
to plasma instability mechanisms can be explored further
through power spectral density analyses. We present in
Figures 4 and 5 just such results for each of the boundaries
in Figure 3 (1E and 1W refer respectively to the eastern and
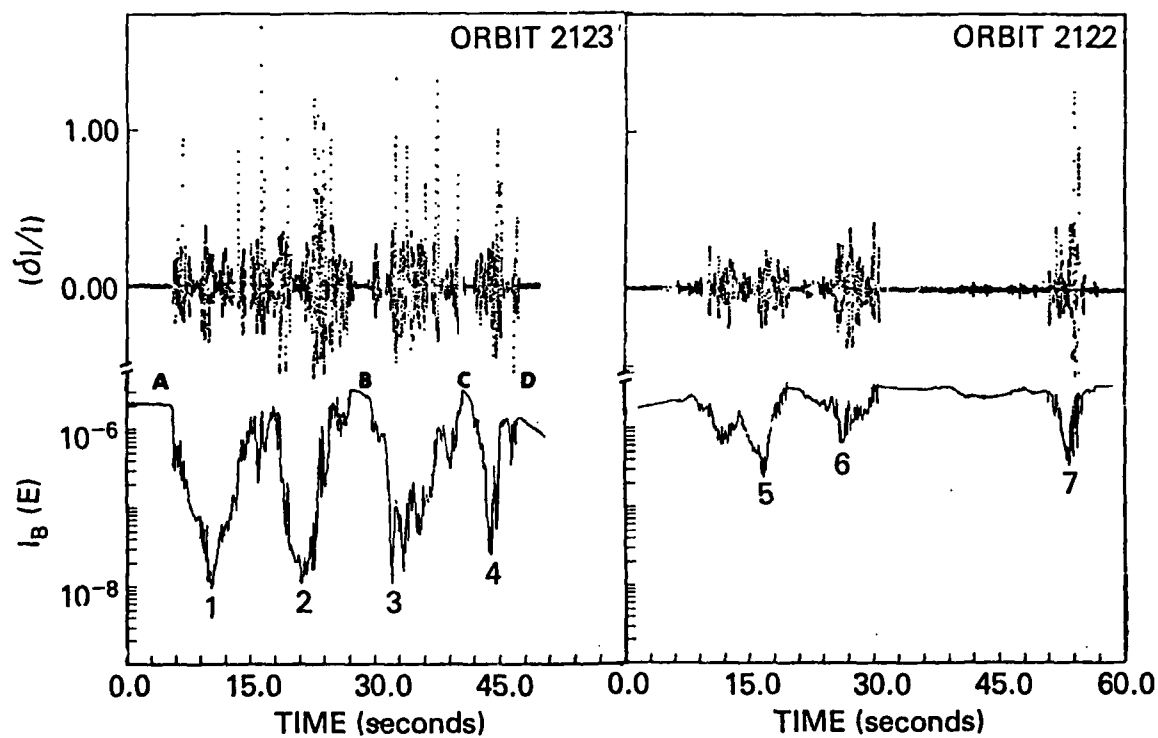western boundary of depletion number 1). Though the experiment

6

Figure 3

The electron density variation (as indicated by $I_B(E)$) for rev #2122 and 2123 along with irregularity intensity ($\delta I/I$) determined over contiguous 2.1 km intervals throughout the depletion.

provides the density fluctuation power spectra with a maximum Nyquist frequency of 400 Hz (19 m resolution along the orbit and 3-5 m resolution perpendicular to magnetic field) the data in this figure has been decimated by a factor of 3 in order to include greater spatial domains across the depletion walls. Power spectral analyses are presented across the boundaries of each of the seven depletions with spectral indices (n, in the equation $P = P_c f^{-n}$) ranging from 1.9 to 2.5. More important however, is the ratio of spectral strengths (entered as $P_1 \equiv P_o(\text{west})/P_o(\text{east})$ in Figures 4 and 5) found to be 1.4 to 11.3 times more intense on the western boundaries. These intensity ratios extend down to a 15 meter wavelength perpendicular to the geomagnetic field. The spectral indices support the work of Keskinen et al. (1980) which predicts the same approximate range of values for horizontal irregularity structures perpendicular to $\bar{B}$. The east-west asymmetry in the depletions is apparent from the linear detrend of data and the ratio of spectral strengths.

We now show that the asymmetry bears on scintillation observations. To do this we note that scintillations depend upon $\Delta N (\Delta N \propto \Delta I)$ rather than $\Delta N/N$ (as calculated by $\underline{(\Delta I)}$ and the power spectral analysis $P_o \propto (\frac{\Delta I}{I})^2$). For the purpose of scintillation-effect calculations, we have determined $|\Delta I|^{r.m.s.}$ in the wavelength domain 80 m to 8 km by assuming that $P^{r.m.s.}$ in this domain is equal to $(|\Delta I|^{r.m.s.}/\bar{I})^2$. Defining P_2 as

$$P_2 = \frac{(\Delta I)_{r.m.s.} \text{ (in the wavelength range 80m-8km on the west wall)}}{(\Delta I)_{r.m.s.} \text{ (in the wavelength range 80m-8km on the east wall)}}$$

we find the values of P_2 ranging from 1.1 to 7.7. These results suggest enhanced scintillation effects on the western wall of the depletions, in agreement with the observations of Livingston et al. (1980). Furthermore, the radar measurements (Tsunoda, 1979) also show that the bottomside backscatter strength is often asymmetric in the east-west plane with stronger backscatter from the western wall of a plume. The combined observations support a model of E-W asymmetry which allows for a neutral-wind driven instability growth rate enhancement on the western side of a rising bottomside F-region depletion. The maximum growth rate occurs on the western wall of the rising depletion, where the electron density gradient is most closely aligned with the plasma drift velocity vector in the reference frame of the neutral wind (Tsunoda, 1979; Zalesak et al. 1980).
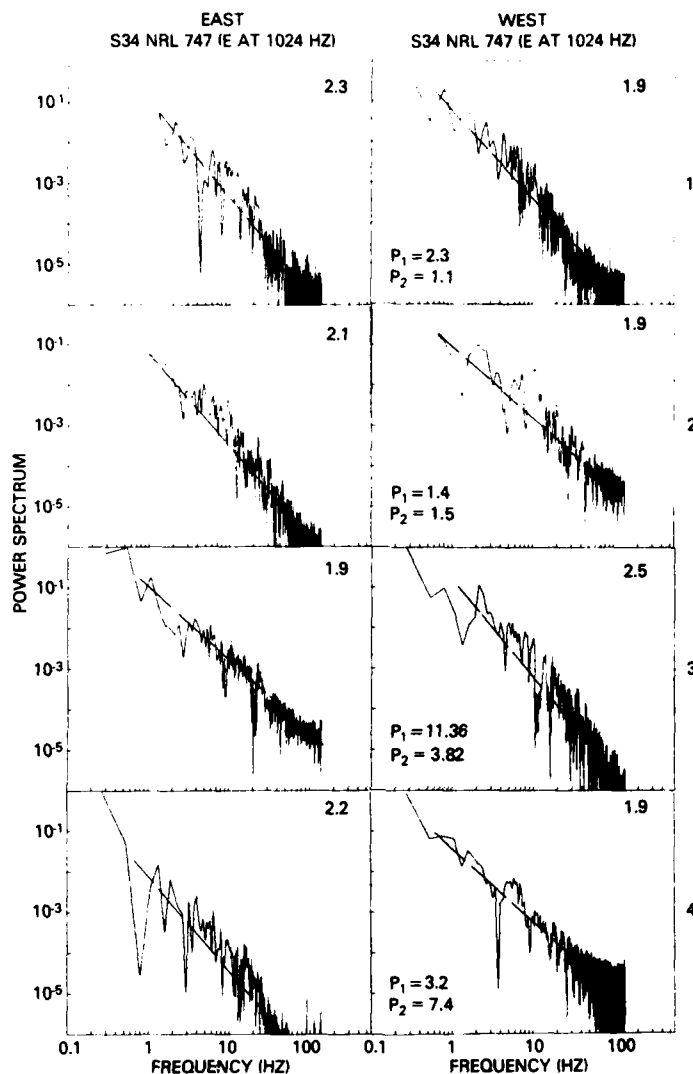
8

EAST
S34 NRL 747 (E AT 1024 HZ)

WEST
S34 NRL 747 (E AT 1024 HZ)

2.3

1.9

1

$P_1 = 2.3$
$P_2 = 1.1$

2.1

1.9

2

$P_1 = 1.4$
$P_2 = 1.5$

1.9

2.5

3

$P_1 = 11.36$
$P_2 = 3.82$

2.2

1.9

4

$P_1 = 3.2$
$P_2 = 7.4$

POWER SPECTRUM

0.1   1   10   100
FREQUENCY (HZ)

0.1   1   10   100
FREQUENCY (HZ)

Figure 4

Power spectral analyses across the boundaries of the
four depletions (1 through 4) of rev #2123 in Figure 3.
The number in the upper right portion of each panel
is the spectral index (n in the equation

$P = P_o k^{-n}$). The value P_1 in each right panel is the
ratio of spectral strengths (P_o) of western to eastern
boundary $P_1 = P_o$ (West)$/P_o$(East). The value P_2 is the
ratio of r.m.s. value of spectral strength in the
wavelength domain (80 m-8 Km) of western to eastern
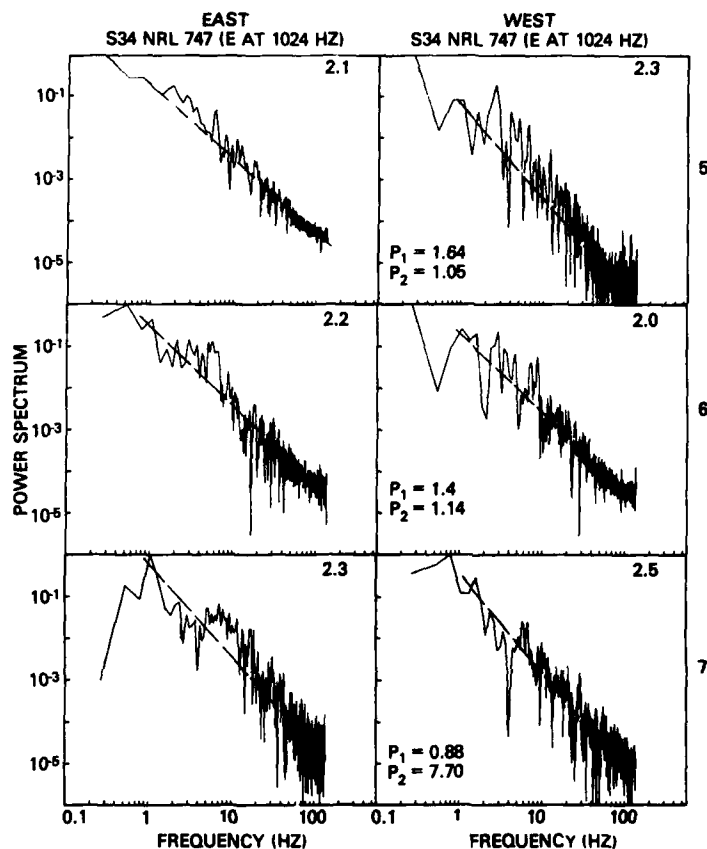boundary ($P_2 = P_{r.m.s.}$ (West)$/P_{r.m.s.}$ (East)).

9

EAST
S34 NRL 747 (E AT 1024 HZ)

WEST
S34 NRL 747 (E AT 1024 HZ)

Figure 5

Power spectral analyses across the boundaries of the
four depletions (5 through 7) of rev #2122 in Figure 3.
The number in the upper right portion of each panel
is the spectral index (n in the equation

$P = P_o k^{-n}$). The value P_1 in each right panel is the
ratio of spectral strengths (P_o) of western to eastern
boundary $P_1 = P_o(\text{West})/P_o(\text{East})$. The value P_2 is the
ratio of r.m.s. value of spectral strength in the
wavelength domain (80 m–8 Km) of western to eastern
boundary ($P_2 = P_{r.m.s.}(\text{West})/P_{r.m.s.}(\text{East})$).

10

COMMENTS AND CONCLUSIONS

The results of the high resolution S3-4 satellite
experiment for equatorial F-region irregularities show large
scale plasma depletions (1 km to 10's of km wide) with
smaller scale irregularities superimposed (smallest detectable
scale size $\sim$ 10 meters perpendicular to $\bar{B}$). The depletions
(which may in fact represent the bottomside upwelling process
that has come to be identified with the lower F-region
manifestations of spread-F) show east-west asymmetry with
the irregularity intensity and spectral strengths generally
more intense on the western boundary. Associated calculations
over density fluctuations in the range 80 meters to 8 km
suggest that scintillation effects would be similarly more
intense on the western boundary. We find these observations
consistent with radar (Tsunoda, 1979) and scintillation
measurements (Livingston et al. 1980) as well as the recent
computational work of Zalesak et al. (1980). Furthermore,
we find the horizontal power spectral indices to lie between
1.9-2.5, supporting the role of Rayliegh-Taylor instability
(Keskinen et al. 1980) and the recent theoretical and experi-
mental comparison in the vertical plane (Keskinen et al.
1981).

REFERENCES

Brinton, H.C. H.G. Mayr, and G.P. Newton, "Ion composition in the nighttime equatorial F-region: Implications for chemistry and dynamics", (abstract) EOS Trans. AGU 56 1038 (1975).

Hanson, W.B. and S. Sanatani, "Large N_i gradients below equatorial F-peak", J. Geophys. Res. 78, 1167 (1973).

Holmes, J.C. and E.P. Szuszczewicz, "A versatile plasma probe", Rev. Sci. Instr. 46, 592 (1975).

Keskinen, M.J., S.L. Ossakow and P.K. Chaturvedi, "Preliminary report on numerical simultations of intermediate wavelength collisional Rayleigh-Taylor instability in equatorial spread-F", J. Geophys. Res. 85, 1775 (1980).

Keskinen, M.J., E.P. Szuszczewicz, S.L. Ossakow and J.C. Holmes, "Nonlinear theory and experimental observations of the local collisional Rayleigh-Taylor instability", J. Geophys. Res. (1981, in press).

Livingston, R.C., E. Weber and T. Bauchau, "Multi-scale observations of irregularities in an isolated and decaying plasma bubble", Paper presented at International Symposium on Equatorial Aeronomy, Aguidilla, P.R., July 1980.

McClure, J.P., W.B. Hanson and J.N. Hoffman, "Plasma bubbles and irregularities in the equatorial ionosphere", J.Geophys. Res. 82, 2650 (1977).

Scannapieco, A.J. and S.L. Ossakow, "Non linear equatorial spread-F", Geophys. Res. Lett. 3, 451 (1976).

Szuszczewicz, E.P., "Ionospheric holes and equatorial spread-F: Chemistry and transport", J. Geophys. Res. 83, 2665 (1978).

Szuszczewicz, E.P., R.T. Tsunoda, R. Narcisi, and J.C. Holmes, "Coincident radar and rocket observations of equatorial spread-F", Geophys. Res. Lett. 7, 537 (1980).

Szuszczewicz, E.P., J.C. Holmes and M. Singh, "The STP/S3-4 ionospheric irregularity satellite experiment", J. Geophys. Res. (1981, submitted).

Tsunoda, R.T., "The growth and decay of equatorial backscatter plumes", DNA report, SRI International, (Nov. 1979).

Tsunoda, R.T., M.J. Baron, J. Owen and D.M. Towle, "Altair: An incoherent scatterradar for equatorial spread-F studies", Radio Sci. 14, (1979).

Woodman, R.F. and C. La Hoz, "Radar observations of F-region equatorial irregularities", J. Geophys. Res. 81, 5447 (1976).

Zalesak, S.T., S.L. Ossakow and P.K. Chaturvedi, "An explanation of westward tilts, fishtails and C's in the equatorial spread-F ionosphere', EOS Trans. AGU 61, 1059 (1980).